Supporting Information

Protein Modification. Ruthenium-modified HiPIPs were prepared by reacting reduced protein (~ 0.1 mM) dissolved in 250 mM $NaHCO_3$/10 mM HEPES (pH 7.7-8.2) with a 3-5 fold excess of $[Ru(bpy)_2CO_3]\cdot 4H_2O$ (in the case of (His18)HiPIP a 1:1 protein-Ru ratio was used). The reactions were quenched by gel filtration. Ru(HisX)HiPIP (X = 18, 42, 50, 81) was isolated by means of two chromatographic (FPLC) steps: (1) Affinity chromatography (IMAC) was performed as described previously (Di Bilio et al., *JACS*, **1998**, *120*, 7551-7556; (2) the material that did not bind to the IMAC column was recovered, equilibrated with 20 mM TRIS buffer at pH 8.1 (buffer A), and separated with a HR 5/5 Mono Q column using a salt gradient (buffer B was 20 mM TRIS/ 300 mM NaCl pH 8.1). However, in most cases a second FPLC run was needed to achieve baseline separation. $Ru(bpy)_2(H_2O)$(His)HiPIPs were identified by their absorption spectra (Figure 1A-B). The yields of protein modified at histidine were moderate in all cases, with the exception of (His18)HiPIP, which afforded $Ru(bpy)_2(H_2O)$(His18)HiPIP in practically 100% yield. $Ru(bpy)_2$(im)(His)HiPIPs were obtained by equilibrating $Ru(bpy)_2(H_2O)$HiPIP$[Fe_4S_4]^{2+}$ with 100 mM im/ 50 mM NaCl (pH 7.0-7.2), and keeping these solutions under argon for 1-2 weeks at room temperature. *Care must be exercised in order to prevent protein denaturation by maintaining the concentration of imidazole ≤ 100 mM.* Samples were repurified before use in laser experiments. No ruthenium coordination to (HisX)HiPIP (X = 20, 48, and 66) was observed.

Absorption Spectra. Absorption spectra were recorded with a Hewlett-Packard Diode-Array spectrophotometer.

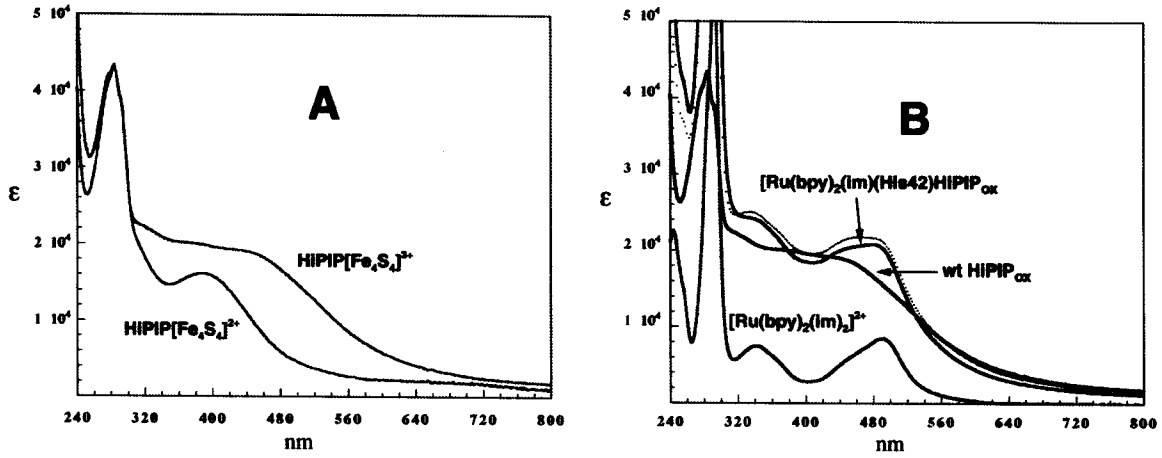

Figure 1. Absorption spectra of reduced and oxidized *wt* HiPIP (**A**). Absorption spectra of *wt* HiPIP$[Fe_4S_4]^{3+}$, $[Ru(bpy)_2(im)_2]^{2+}$, and $Ru(bpy)_2$(im)(His42)HiPIP$[Fe_4S_4]^{3+}$; the dotted line represents the overlap of the absorption spectra of *wt* HiPIP and $[Ru(bpy)_2(im)_2]^{2+}$ (**B**).

Reduction Potentials. Reduction potentials were measured by cyclic voltammetry (Figure 2A-D, Table 1) using a Potentiostat/Galvanostat PAR model 273A. A pyrolitic graphite disk (PGE) was used as working electrode, and saturated calomel and Pt electrodes were used as a reference and counter electrode, respectively. Electric contact between the reference electrode and working solution was achieved with a Wycor set. All measurements were carried out under argon (the medium was NaPi, μ = 0.1 M, pH 7.0) and thermostatic control, at scan rates in the range 0.02 to 0.2 V/s. The temperature dependence of the reduction potential was determined with a "nonisothermal" cell, in which the reference electrode was kept at constant temperature while the temperature of the working electrode was varied. Anodic and cathodic peak currents were almost identical and proportional to protein concentration and $v^{1/2}$ (v = scan rate), indicating a reversible (or quasi-reversible) electrochemical processes. The cleaning procedure of the PGE electrode was crucial to the voltammetric response: the PGE was first treated with anhydrous ethanol for 10 min, polished with alumina (BDH, particle size ~ 0.015 μm) water slurry on cotton wool for 3 min, and finally treated in an ultrasonic pool for about 5 min.

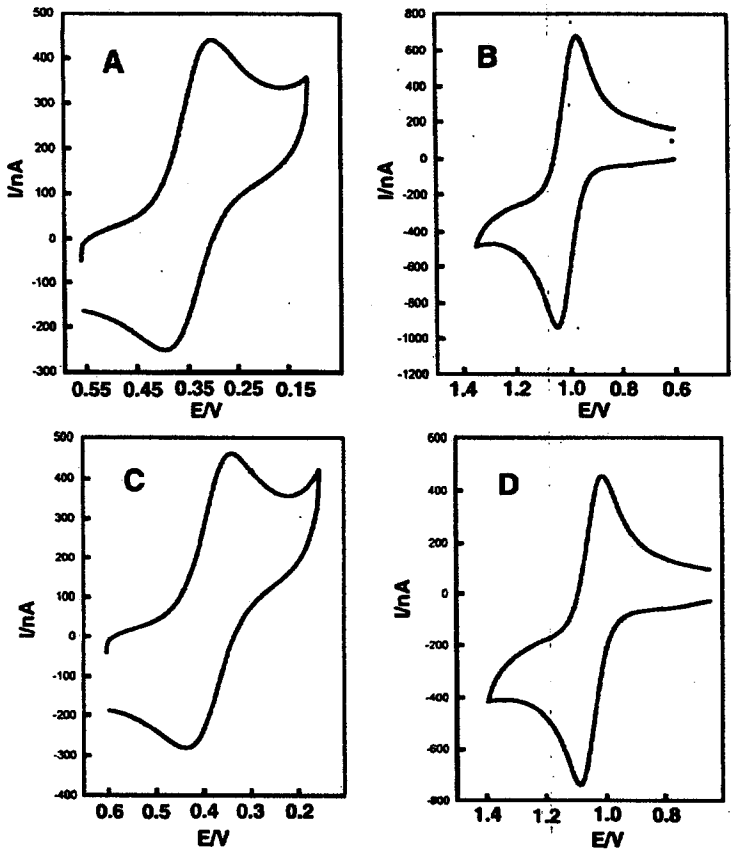

Figure 2. Cyclic voltammograms for native HiPIP (**A**), $[Ru(bpy)_2(im)_2]^{2+}$ (**B**), and $Ru(bpy)_2(im)$(His42)HiPIP (**C-D**).

Table 1. Reduction potentials (vs NHE) as a function of temperature for the $[Fe_4S_4]^{3+/2+}$ and $Ru^{3+/2+}$ couples of $Ru(bpy)_2(im)$(His42)HiPIP.

T (K)	HiPIP$[Fe_4S_4]^{3+/2+}$	RuHiPIP$[Fe_4S_4]^{3+/2+}$	$Ru^{3+/2+}$HiPIP	$-\Delta G°$(eV)
278.2	0.363	0.393	1.040	0.647
283.2	0.361	0.390	1.043	0.653
288.2	0.359	0.388	1.043	0.655
293.2	0.355	0.386	1.045	0.659
298.2	0.353	0.384	1.046	0.662
303.2	0.352	0.381	1.048	0.667
308.2	0.348	0.378	1.050	0.672
313.2	0.347	0.376	1.051	0.675

Electron Transfer. ET could be monitored at any wavelength in the range 300-600 nm: $\Delta\varepsilon(\text{red-ox})_{HiPIP}$ ~ -10,800 $M^{-1}cm^{-1}$ (478 nm) (Bartsch, R. G. *Methods Enzymol.* **1971**, *23*, 644-649); $\Delta\varepsilon(\text{ox-red})_{Ru}$ ~ -7,000 $M^{-1}cm^{-1}$ (492 nm), and $\Delta\varepsilon(\text{ox-red})_{Ru}$ ~17,500 $M^{-1}cm^{-1}$ (316 nm) (Figure 3A-B). Excitation of $Ru(HisX)^{2+}$-$HiPIP_{ox}$ gives $*Ru(HisX)^{2+}$-$HiPIP_{ox}$; intramolecular oxidative quenching yields $Ru(HisX)^{3+}$-$HiPIP_{red}$, which undergoes $[Fe_4S_4]^{2+} \rightarrow Ru(HisX)^{3+}$ ET (Figure 4A-C).

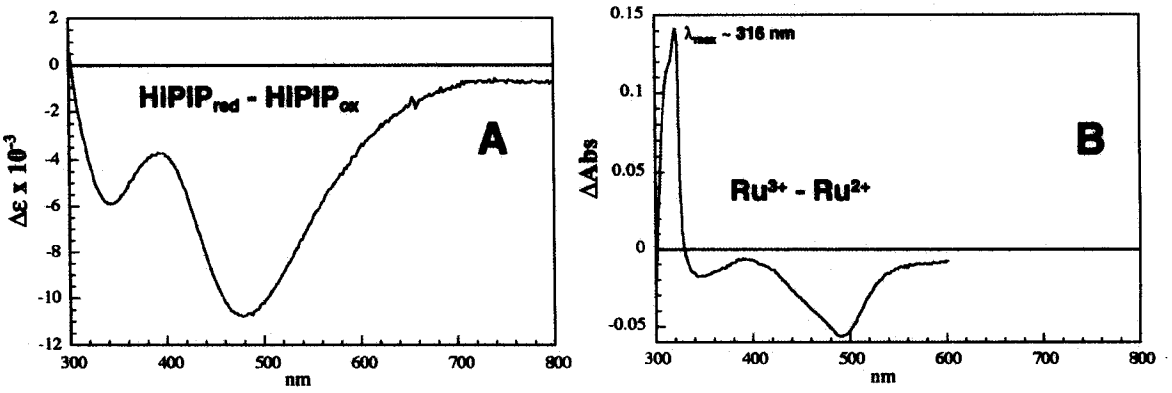

Figure 3. HiPIP difference (reduced minus oxidized) absorption spectrum. (**A**). Ruthenium difference ($[Ru(bpy)_2(im)_2]^{3+}$ minus $[Ru(bpy)_2(im)_2]^{2+}$) absorption spectrum (**B**).

Figure 4. ET scheme (**A**). Transient absorption kinetics of a ~100 μM solution of Ru(dmbpy)$_2$(im)(His42)-HiPIP$[Fe_4S_4]^{3+}$ (λ_{ex} 355 nm, 1 mJ, 10 ps FWHM; λ_{obs} 532 nm. The continuous line is the best fit to a double-exponential function (**B**). Transient absorption kinetics of a solution of Ru(bpy)$_2$(im)(His50)-HiPIP$[Fe_4S_4]^{3+}$ (~ 30 μM in μ = 0.1 M NaP_i, pH 7.0, 22 °C) (**C**). The panel shows the kinetics monitored at 431 nm (an isosbestic point for $[Ru(bpy)_2(im)(His)]^{2+}$ and its MLCT excited state), following excitation with a 480 nm laser pulse (1-2 mJ/pulse, FWHM ~ 25 ns). The heavier line is the best fit to a single-exponential function: the fitting procedure yielded a $[Fe_4S_4]^{2+} \rightarrow Ru^{3+}$ rate constant equal to 1.8(2) x 10^6 s^{-1}. The same rate constant was obtained at 316 and 580 nm. The residual ~ 0.02 ΔOD at 4 μs is due to a small amount of Ru(bpy)$_2$(OH)(His50)$^{2+}$-HiPIP$[Fe_4S_4]^{2+}$